Examination of Pore Characteristics and Behavior of Gas and Water Permeability in Blast Furnace Slag Concrete

T. Iyoda[1*], and A. Shibuya[2]

[1] *Shibaura Institute of Technology, Tokyo, Japan*

Email: iyoda@shibaura-it.ac.jp
[2]*Tobishima Corporation, Chiba, Japan*

Email: Akari_Shibuya@tobishima.co.jp

ABSTRACT

In consideration of reduction for environmental impact, the use of mixed cement is indispensable for construction. In Japan, blast furnace slag cement using ground granulated blast furnace slag fine powder is mainly used, and blast furnace slag cement with a replacement rate of about 45% is mainly used for civil engineering structures. On the other hand, the use of blast furnace slag cement with a replacement rate of about 70% has been studied with the aim of further reducing the environmental impact. From previous studies, it is known that concrete using blast furnace slag cement has a dense pore structure. However, the total pore volume of the cured blast furnace slag cement concrete is not significantly different from the concrete using ordinary Portland cement. In this study, it will be clear the relationship between pore structure and gas and moisture permeability. As a result, the water permeability of blast furnace slag cement concrete is significantly improved as compared with concrete using ordinary Portland cement. On the other hand, a result of gas permeability was little difference compared these different cement concrete. This is a result showing that although there is no difference in the total amount of pores, the permeation performance using highly viscous water is significantly different, and it can be said that this represents a great feature of blast furnace slag cement concrete.

KEYWORDS: *Blast furnace slag cement, gas permeability, water permeability, pore structure*

1. Introduction

Durability is particularly important in the performance required of reinforced concrete structures. In the required durability of reinforced concrete structures, steel corrosion and concrete deterioration are to be conducted. The steel corrosion is the main cause of deterioration of reinforced concrete structures in Japan. Since steel corrosion progresses by the supply of water and oxygen, it is important to understand the material permeability in concrete. Concrete has porous structure, and materials move through its connected pores. However, pores of different sizes and shapes are intersected and connected in a complex, and it is difficult to represent the movement of degradation factors in a simple model.
Therefore, it was important to directly understand the material permeability resistance from the results of mass transfer tests. In the evaluation of mass transfer resistance in concrete, it is often discussed together with durability because some materials react with cement hydrate or adsorbed in the pores. Specifically, carbonation, which considers the movement and reaction of carbon dioxide, and salt damage, which discusses the movement, immobilization, and adsorption of chloride ions. In durability tests, mass transfer and reaction are discussed at once, but in this study, we focused only on the material permeability resistance due to differences in the structure of pores. In this study, we focused only on the mass transfer in order to understand the material permeability resistance in different pore structures.
On the other hands, recently, the use of admixtures has been increasing due to the demand for structures to reduce environmental impact and improve durability. In Japan, the mainly use of large quantities of

blast furnace slag fine powder has been attracting attention. However, it is not cleared the model for proposed these materials because it has a complexed pore structure.
The pore structure is considered to have a significant effect on the material permeability and is important for understanding the durability. Therefore, in this study, cured materials were generated using various powders, and mass transfer tests were conducted. In order to change the driving force, we conducted permeability tests and air permeability tests using pressure as the driving force, and capillary force as the driving force on water permeability test. The purpose of this study was to clarify the pore structure and mass transfer characteristics.

2. Outline of mortar test

In this section, tests were conducted using mortar in order to clear the pore structure formed by various admixing powders on the mass transfer test., eliminating voids such as interfacial transition zone affected by coarse aggregate.

2.1 Materials used and specimen specifications

Table 1 shows the mix proportions for mortar and the compressive strength of each mix proportions after 28 days in tap water. The water-binder ratio was set at 0.5 and the weight ratio of binder to fine aggregate was kept constant at 1:3. Ordinary Portland cement (OPC, density 3.16g/cm^3, Blaine 3080 cm^2/g) was used as cement, and mixed sand (surface dry density 2.60 g/cm^3, water absorption ratio 1.92%, coarse-grained ratio 2.62) was used as fine aggregate. As admixture, blast furnace slag fine powder (B, density 2.91g/cm^3, Blaine 4190 cm^2/g, with gypsum addition), fly ash type II (JIS A 6201), (FA, density 2.33g/cm^3, Blaine 4460 cm^2/g), and silica fume (SF, density 0.27g/cm^3, Blaine 18.5m^2/g) were used. The specimens were demolded on the day after casting and cured in water until 28 days. Specimen size is decided depending for testing methods as 40 x 40 x 160 mm for compressive strength (JIS R 5201) and porosity, φ50 x 100 mm for moisture penetrating test and φ100 x 20 mm for air permeability test.

Table 1 Mix proportions for mortar and compressive strength at 28days

	W/B	Weight ratio (%)		Compressive strength (N/mm^2)
		OPC	Blended powder	
N	0.5	100	-	49.6
B20		80	20	47.5
B30		70	30	49.3
B50		50	50	44.8
B70		30	70	41.1
B90		10	90	15.9
FA10		90	10	46.7
FA30		70	30	36.9
SF10		90	10	47.2
SF30		70	30	44.9

2.2 Testing methods

(1) Porosity test
The porosity of various mix proportions was calculated by the Archimedes method. After 28 days of curing in water, about 40 x 40 x 30 mm was cut from the specimen, and the specimen was kept under reduced pressure of -0.1 MPa for 12 hours with the specimen in water, and the pores were filled with water to measure the mass of saturated water and mass in water. The pores were filled with water and the saturated mass and the mass in water were measured. Acetone was used to stop hydration, and the pores were left in a constant volume at 40°CRH30%.

(2) Moisture evaporating test
40 x 40 x 160 mm specimen was cured in water, the water on the surface was wiped off, and the specimen was placed on a constant temperature and humidity chamber at 20 degrees Celsius and 60% Relative Humidity. The water was allowed to evaporate from all surfaces except the bottom of the 40 x 160 mm specimen, and the mass change was recorded over time.

(3) Air permeability test
Air was injected at a pressure of 0.05 MPa, and the amount of air permeating through the mortar was measured by the water displacement method after confirming that the air permeated through the mortar reached a steady state. After that, the pressure was increased to 0.1 MPa in the same specimen and the permeability test was conducted in the same way. The permeability coefficient was calculated using Darcy's rule in Equation (1).

$$K = \frac{2LP_2}{P_1^2 - P_2^2} \times \frac{Q}{A} \tag{1}$$

where K: permeability coefficient ($cm^4/(N\text{-}s)$), L: specimen thickness (cm), P1: loading pressure (N/cm^2), P2: outlet pressure (0.1 N/cm^2), Q: permeability (cm^3/s), A: permeable area (cm^2)

(4) Moisture penetration rate coefficient test
The test was conducted in accordance with JSCE-G 582-2018 in showing Figure1. The test specimens were dried at 40 degrees Celsius and 30% Relative Humidity for 28 days, and the sides were sealed with aluminum tape to make two open sides. The specimens were immersed up to a height of 1 cm from the bottom of the specimen, removed at 5, 24, and 48 hours after immersion, and after measuring the mass, the specimens were split and sprayed with a moisture sensing agent to measure the depth of coloration. The moisture penetration rate coefficient was calculated from the change in moisture penetration depth over time. In the experiment, pumped water was used in consideration of the effect of air.

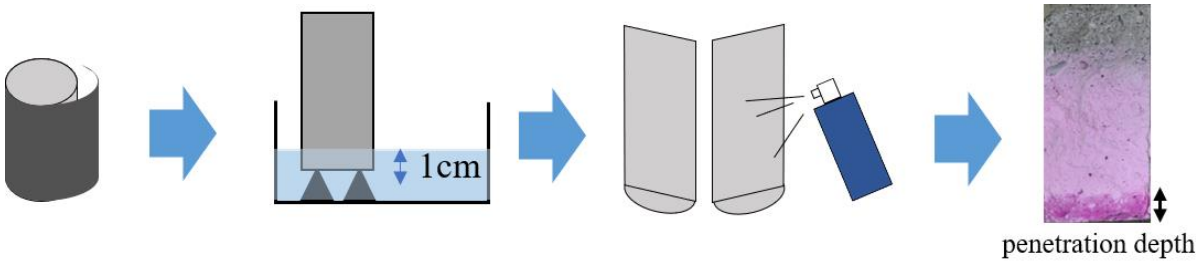

Figure 1. Outline of moisture penetration test (JSCE-G 582)

2.3 Test results

(1) Porosity and Moisture Evaporating Test
Figure 2 shows the porosity of the various specimens. Since the porosity is calculated by Archimedes method using water, it is considered to be the total amount of porosity that water can move through, and the amount of porosity that water can move through is small in B50 and B70. On the other hand, the value of B90 was larger than that of other blends using blast furnace slag powder. This is because B90 showed a very small value in the compressive strength in Table-1, and it is highly possible that the blast furnace slag powder did not react sufficiently. FA10, FA30, SF10, and SF30 showed comparable and larger porosity than N, suggesting a larger amount of porosity for water to move through.
Here, as shown by Sagawa (2010), capillary water is defined as the water evaporated at 40 degrees Celusis drying, and gel water as the water evaporated between 40 degrees Celusis and 105 degrees Celusis. In the porosity measurement by Archimedes method, it is calculated by using the mass of the pore filled with water and the mass dried at 40 degree Celusis. Since gel water remains, it is considered to

be the porosity up to the capillary pore. On the other hand, based on the amount of water evaporation at 20 degrees Celusis and 60% Relative Humidity, we can calculate the wet porosity ratio, which captures the pore space larger than the capillary pore. The wet porosity ratio was calculated by Equation (2), dividing the difference between the mass of the specimens immediately after curing in water and the mass at 960 hours, when the mass of all specimens was approximately constant, by the volume of the pores in which water had dissipated at 20 degrees Celusis, and dividing the results by the volume of the specimen.

$$\text{The wet porosity ratio} = (m1 - m2)/V \quad (2)$$

Where, m1: the mass of the specimens immediately after curing in water
m2: the mass after standing for 960 hours at 20 degrees Celsius and 60% Relative Humidity
V: the volume of the specimen

Figure 3 shows the relationship between the porosity and the wet porosity ratio, and the wet porosity ratio of SF, FA, and B30 is smaller than that of the others. It is known that silica fume has extremely few pores larger than 0.1 μm, and it is thought that the difference in the pore network could be expressed by comparing the results between the results of all samples.

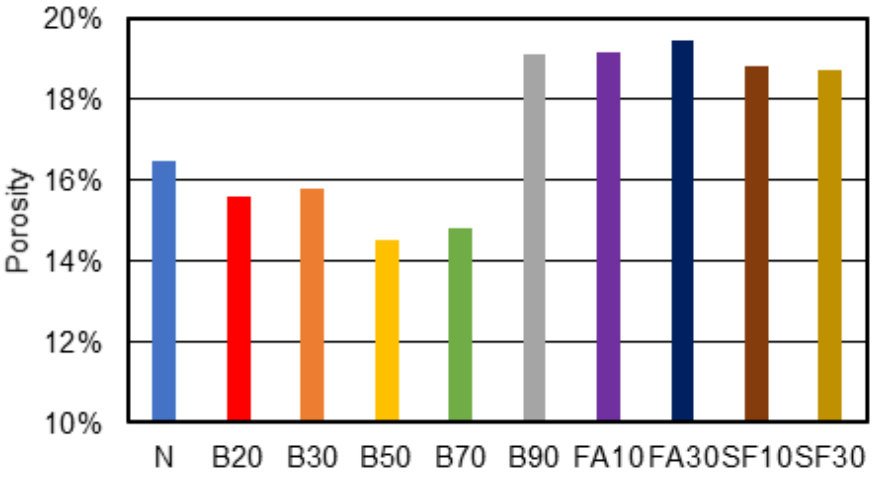

Figure 2. Porosity od different mix proportions

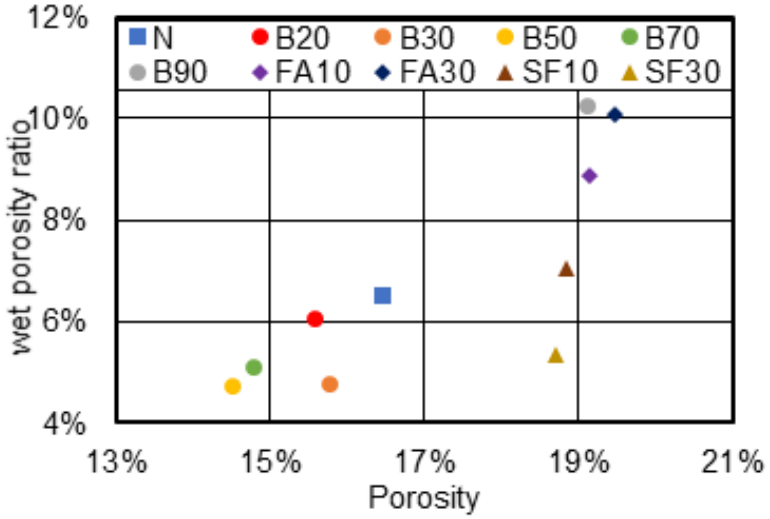

Figure 3. Relationship between porosity and wet porosity ratio

(2) Air permeability test

Figure 4 shows the air permeability coefficients calculated from the air permeability tests conducted at pressures of 0.05 MPa and 0.1 MPa. The air permeability coefficients are almost the same even though the pressures are different, indicating that the mass transfer at different pressures follows the Darcy law even though the pore networks are different. Therefore, the air permeability indicates the flow pattern of the steady state flow, and the smallest value was observed for B30, which indicates that it has a dense pore network with few continuous pores. The trend of air permeability in FA and SF was also confirmed by Ujike(1986). in concrete, where it was shown that the air permeability became much lower after 91 days of curing in water, and the mass transfer test in long-term curing should be studied in the future. Since the air permeability was reduced by mixing the appropriate amount of pozzolanic material, it can be assumed that the reduction in air permeability was achieved by filling the capillary pores with hydration products from the pozzolanic reaction.

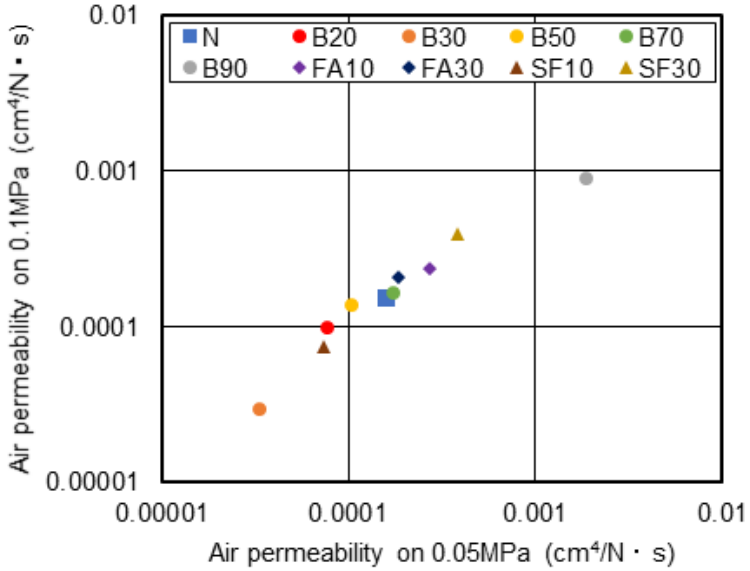

Figure 4. compare to the air permeability on different puressures

(3) Moisture penetration coefficient

Figure 5 shows the moisture penetration rate coefficient as a bar graph (left axis) and the increasing weight after 24 hours of penetration as a cross mark (right axis). The increasing weight was considered to be the amount of water penetrated, and using B suppressed the penetration more than N, especially B50; FA and SF showed small values at 10% substitution. Kamada(2017) conducted a penetration test of liquid water using microchannels of various shapes and reported that the presence of bubbles and unsaturated regions at the intersections of the channels significantly suppressed the penetration. It was found that the presence of bubbles and unsaturated regions at the intersections of the flow paths greatly suppressed the permeation. B90 showed a relatively large value in the water infiltration rate coefficient, but the water infiltration rate was small, suggesting that the water infiltrated into the field with a bending continuity rather than a linear continuity.

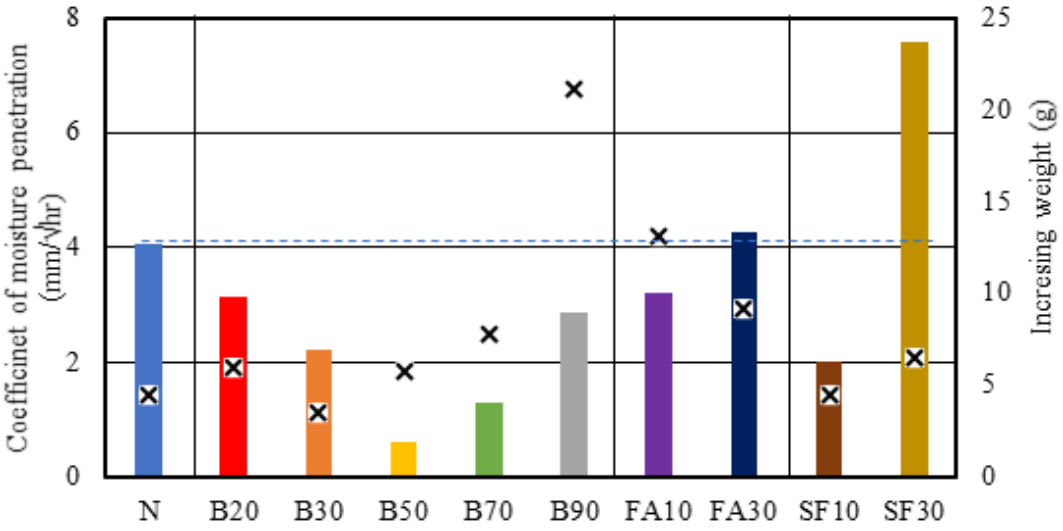

Figure 5. Results of coefficient of moisuture penetration and incrrising weight

3. Outline of concrete test

In this section, material permeability tests were conducted using concrete specimens with varying curing temperatures. In this study, the influence of the interface between the concrete and the aggregate is investigated based on the results of Chapter 2.

3.1 Concrete mix proportions and specimen outline

Table 2 shows the mix proportions of the concrete in this study. Ordinary Portland cement (N) was used to make the concrete with 0, 30, 50 and 70% replacement of blast furnace slag fine powder.
The specimen size was φ100×200mm. The curing is controlled that normal temperature at 20 degree Celsius and high temperature at early age as hydration heat, because we focus on the interfacial tradition zone on different cement type and curing temperatures. Early temperature sets for 40 degrees Celsius and 60 degrees Celsius during 2days from casting concrete.

Table 2 Mix proportions for concrete test

	W/C	Air (%)	s/a (%)	Unit weight (kg/m^3)				
				W	OPC	BFS	S	G
N	0.5	4.5	48	170	340	-	852	952
B30					238	102	848	947
B50					170	170	846	944
B70					102	228	843	942

3.2 Outline of the test

The moisture penetration test and air permeability test were conducted as same methods of Chapter 2. In each test, the specimen size was set to φ100mm in consideration of the influence of coarse aggregate. The several specimens of about 20 mm square were taken from the concrete after the moisture penetration test for porosity test, and the porosity was calculated by Archimedes method. At the same time, mortars of the same mix were prepared and the porosity of each mix proportions was also measured. In the case of concrete containing coarse aggregate, the interfacial transition zone around the coarse aggregate is considered to have a significant effect on mass transfer resistance, and the purpose of this study was to compare the results with those of the base mortar.

3.3 Test results

(1) Moisture penetration and permeability test

Figure 6 shows the change in water penetration depth with time for each cement type. N was a slight tendency for the moisture penetration rate to slow down as the curing temperature increased. For B50, no difference was observed with temperature. On the other hand, B70 showed a small moisture penetration rate at 20 Degree Celsius, but a remarkably large moisture penetration rate at higher temperatures.

Figure 7 shows the relationship between the moisture penetration rate coefficient and the air permeability coefficient of concrete on all mix proportions. N and B30 showed no difference in air permeability coefficient with different temperature and were almost the same. For B50, there was no difference in the moisture permeability coefficient with temperature, but the air permeability coefficient at high temperature was slightly larger. Furthermore, for B70, the moisture penetration rate and air permeability coefficients of high temperature as 40 and 60 degrees Celsius at early age were significantly larger at constant temperature as 20 degrees Celsius.

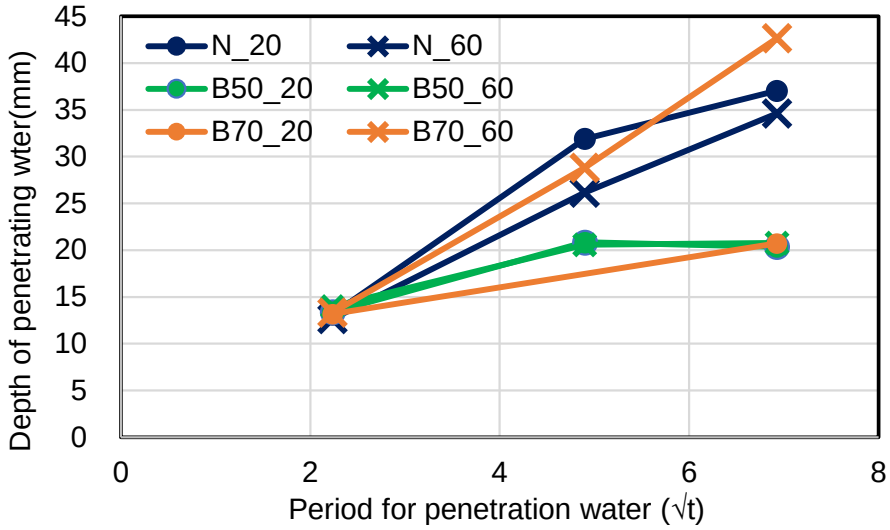

Figure 6 Result of moisture penetrating test on different concrete

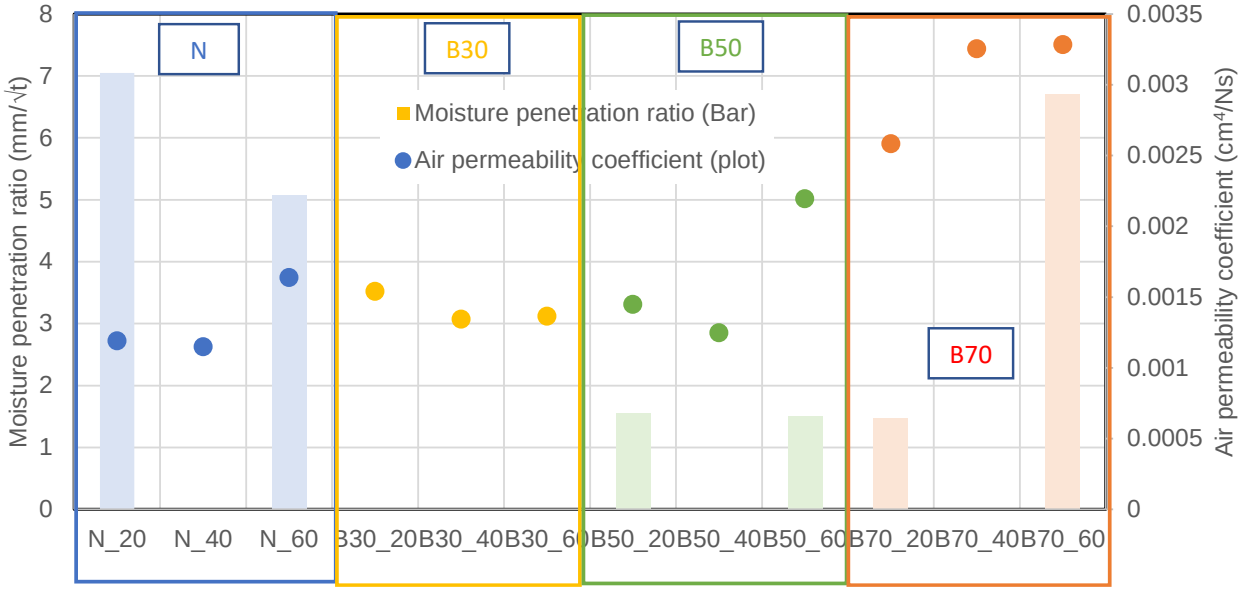

Figure 7 Comparing the results of moisutre penetration ratio and air permeability test

(2) Porosity and air permeability

Figure 8 shows the relationship between the porosity of concrete and mortar on different temperature history. Therefore, the porosity per unit mortar is calculated from concrete porosity and compared with that of mortar, assuming that there are no voids in the coarse aggregate and that the voids around the coarse aggregate are mixed into the mortar. It was confirmed that the porosity of the mortar itself increased with temperature history in N and B30, B50. On the other hand, in the case of B70, the porosity of the mortar itself did not change with the temperature history. However, the porosity per unit mortar in the concrete increased. In the case of B70, it can be inferred that the interfacial transition zone around the coarse aggregate was generated by the temperature history. Figure 9 shows the relationship between the unit mortar porosity and air permeability in concrete. The porosity per unit of mortar is not significantly different between N and B70, but the air permeability of B70 increases with temperature history. This may be due to the formation of interfacial transition zone in B70 at high temperature.

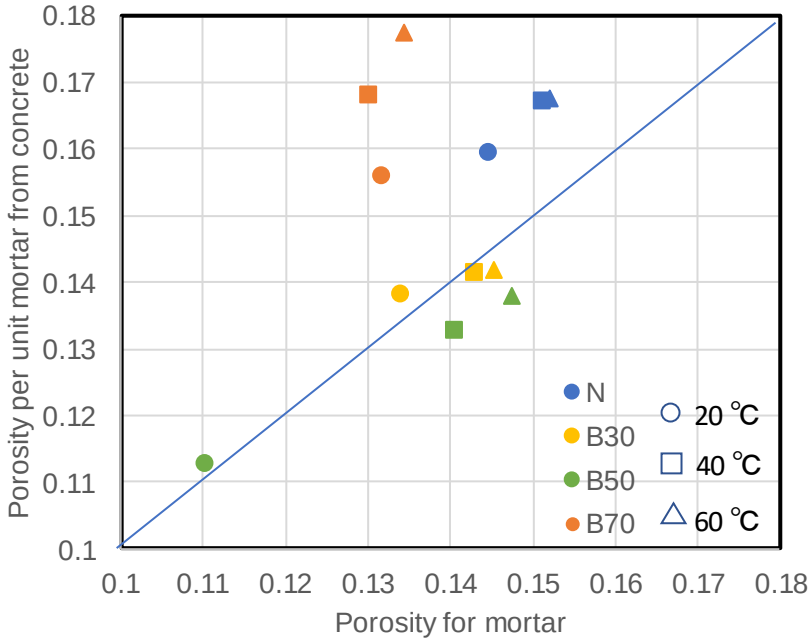

Figure 8. Compare Porosity on mortar and Concrete

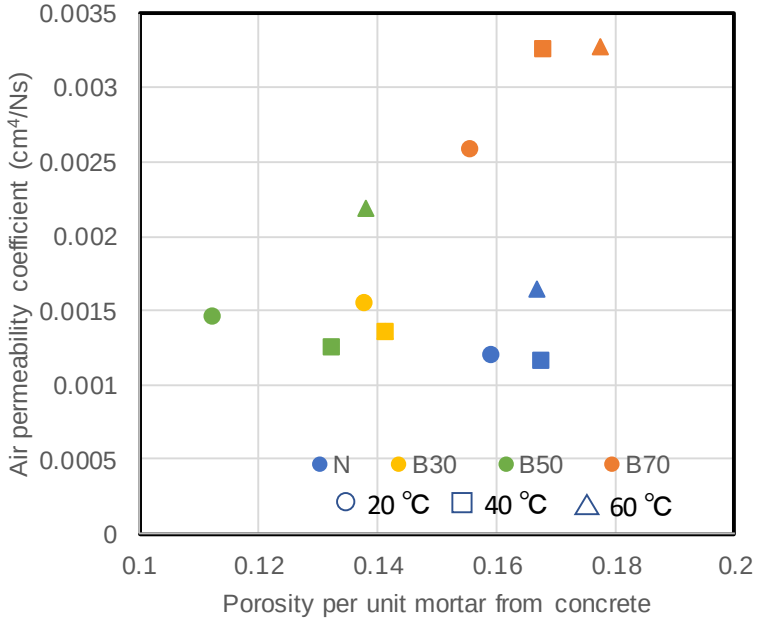

Figure 9. Relationship between porosity and air permeability coefficient

4. Conclusions

The results obtained in this study are summarized as follows.

1) Concrete substituted with blast furnace slag powder becomes complex pore structure and watertight after curing.
2) When blast furnace slag powder is used, the total porosity can be evaluated in gas permeability, but not in moisture permeability test.
3) In the future, it is necessary to clarify the difference between liquid and gas permeability in terms of material permeability and pore structure.
4) By increasing the curing temperature, the formation of transition zone increases in B70, which has a great influence on mass transfer resistance. Because the cement hydration is quickly and stop due to lack of water for hydration. This phenomenon needs more research.

Acknowledgements

Mr. Fukazawa who a graduated student, assisted our experiments in this research. We also received support from the Nippon Slag Association and Grants-in-Aid for Scientific Research (C).

References

Takahiro Sagawa, Tetsuya Ishida, Yao LUAN, Toyoharu Nawa (2010) "Analysis of water and material composition and void structure characteristics of blast furnace cemeteries", *Proceedings of the Civil Engineering Society E*, Vol. 66, No. 3: 311-324 *(In Japanese)*

Isao Ujike, Shigeyoshi Nagataki (1983) "Quantitative Evaluation of Air Permeability of Concrete", *Proc. of JSCE*, No.396: 79-87 *(In Japanese)*

Isao UJIKE, Masanao NARAZAKI and Shigeyoshi NAGATAKI (1993) "Study on Permeability of Concrete and Diffusion of Oxygen and Chlorine Ion", *Proc. of the JCI*, Vol.15, No.1 *(In Japanese)*

Tomohisa Kamada, Toshiharu Kishi (2017) "A Study on the Controlling Factors of Resistance to Liquid Water Penetration into Cement Hardened Paste", *Proc. of the JCI*, vol.39, No.1 *(In Japanese)*

Iyoda et al.(2005) "Temperature Dependent Properties of Cement with High Blast Furnace Slag Powder Content", *Proc. of the JCI*, vol.27, No.1 *(In Japanese)*

Takeshi Iyoda, Takahiro Kameyama and Yoko Harasawa (2016) "A Study on Understanding The Hydration Reaction of Blast Furnace Cement Focus on The Amount of Water Consumed", *The 7th International Conference of Asian Concrete Federation "Sustainable Concrete For Now and The Future"*, CD-ROM

Takeshi Iyoda (2016) "Comparison for permeability resistance between concrete and mortar", *The Fifth International Symposium on Life -Cycle Civil Engineering, IALCCE2016*: 1304-1311